SiON high-refractive-index waveguide and planar lightwave circuits

G.-L. Bona
R. Germann
B. J. Offrein

The rapidly growing optical communication market requires photonic components with ever-increasing functionality and complexity that can be fabricated reliably at low cost. Of the various approaches used to fabricate photonic components, those based on planar waveguides have achieved high performance and represent a promising path toward compact integration of optical functions. We present an overview of an approach used to produce an optical single-mode waveguide. Through its strong mode confinement, the approach makes it possible to integrate optical filter functions with higher functionality, as required for high-data-rate communication networks. The waveguide is based on the use of a silicon oxynitride (SiON) core and silicon oxide cladding layers, and can be fabricated using conventional chip fabrication techniques. Using the new approach, conventional passive optical components such as arrayed waveguide gratings for wavelength-division-multiplexed transmission systems can be fabricated in a more compact way than using standard silica-on-silicon waveguide methods. Moreover, the realization of more enhanced, adaptive optical functions such as finite-impulse-response as well as infinite-impulse-response filters is possible. Reconfiguration is achieved through the thermo-optic effect. A reconfigurable gain-flattening filter and an adaptive dispersion compensator are presented as examples.

Introduction

The transmitted data capacity in optical communication systems has grown tremendously in the past years to fulfill the needs of the rapidly expanding telecommunication market, where the transport of data now substantially exceeds the aggregate data rate of telephone and voice. Time-division-multiplexed systems have increased from 622 Mb/s to 2.5 Gb/s, and 10 Gb/s; even the wide deployment of 40-Gb/s systems is within reach for network backbones. Furthermore, wavelength-division multiplexing (WDM) with large channel counts offers extensions of the capacity in existing fiber systems [1]. WDM transmission systems are widely deployed in wide-area networks (WANs), and are now beginning to enter metropolitan-area network (MAN) and customer-premises network areas [2, 3]. Most of the optical links still are point-to-point in terms of configuration with the occasional optical WDM add/drop functions, but more advanced ring structures that also employ optical WDM add/drop functions are beginning to appear. In the future, fully meshed, optically transparent networks will be required with high-complexity optical-cross-connect features [4]. This evolution is driven by the requirements for flexibility in photonic network nodes, in particular by the need for optical transparency, because the majority of the traffic in a node is pass-through [5]. The term *optical transparency* denotes the state in which data streams are kept in the photonic domain and redirected through optical switches. Electrical termination of all channels at each node is simply too inefficient, requiring a receiver/transmitter pair

0018-8646/03/$5.00 © 2003 IBM

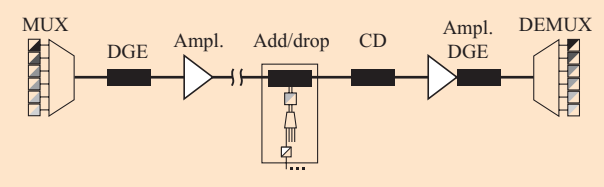

Figure 1

WDM subnetwork for long-haul transmission and routing for point-to-point system. Besides the key functions of opto-electronic conversion and WDM demultiplexing (DEMUX) and multiplexing (MUX), additional functions such as gain equalization (DGE), optical amplification (Ampl.), and compensation of chromatic (CD) and polarization-mode dispersion are required. The WDM-add/drop multiplexer may be fixed or reconfigurable in wavelength.

for each WDM channel. Development is gated by the availability of the necessary optical building blocks, ideally manufactured in large quantities and at low costs. All network applications require optoelectronic conversion elements such as (tunable) lasers and receivers for individual wavelength channels. In addition to these electro-optical components, simple short-distance, low-data-rate, point-to-point WDM transmission systems merely require wavelength multiplexers and demultiplexers at both ends; however, the complexity of these optical functions increases for longer distances and higher data rates. Optical amplifiers make possible transmission over longer spans but have nonlinear gain, and hence need dynamically reconfigurable gain-flattening filters when cascaded to cover long transmission spans of, say, several hundreds of kilometers. Optical WDM add/drop multiplexers allow the insertion and extraction of one or more wavelengths at any arbitrary point in a transmission span. They can be fixed in terms of the wavelength, but there is a growing need for reconfigurable wavelengths to respond to changing needs in network load. To achieve full flexibility, optical switching and WDM channel-equalization functions must be included. Optical signals transmitted over fibers suffer from chromatic and polarization-mode dispersion (CD and PMD), both of which can be compensated passively in specialty fibers at low data rates but require active compensation schemes for WDM transmission at 10 Gb/s or even 40 Gb/s over long distances. Active polarization mitigation is necessary to compensate for temporal instabilities in the network, such as temperature-induced variations of stresses in fibers. The optical functions discussed are schematically shown in **Figure 1** for a point-to-point transmission system. Accordingly, ring networks are constructed using the same optical functions. Cascading such ring networks in a mesh structure leads to general network configurations with optical cross-connects at the connection points.

Although many different technological device solutions are currently employed, it is most likely that diversity will be reduced in the future. With the exception of optoelectronic conversion, high-speed modulation, and full optical pulse regeneration, all of the elements can be integrated cost-effectively in planar lightwave circuits (PLCs) based on glass-type waveguide structures with thermo-optical and/or micro-mechanical reconfiguration features. The exceptions given above will require devices made with III–V semiconductor compounds—for example, InP-based components for lasers, converters, and receivers in the wavelength regime above 1 μm. In principle, all optical building blocks for telecommunication applications can be integrated in InP-based material, but economic considerations continue to favor low-cost planar glass-based PLCs fabricated using conventional chip-manufacturing techniques. Optical hybrid packaging of III–V devices and other elements, such as $LiNbO_3$ modulators or liquid-crystal-based optical phase shifters on planar waveguide optical bench elements in a combined module, will play an important role in reducing costs while maintaining or even increasing performance. In today's performance- and quality-dominated telecommunication environment, although individually handmade components with actively aligned fibers are often formed from bulk optical building blocks such as lenses, prisms, and gratings inscribed in glass blocks with free-space optical propagation, guided wave elements are increasingly being used. For example, the WDM multiplexer component can be realized with excellent performance on planar waveguides in the form of a phased array grating multiplexer [6]. Several companies manufacture such multiplexers with channel counts of 16, 32, or 40, and a wavelength spacing of 100 GHz (0.8 nm at 1550 nm). The vast majority of these passive optical components are fabricated using planar optical-waveguide fabrication processes that match the geometrical mode diameter and refractive index contrast of standard single-mode optical fibers [7–9]. In these conventional approaches, silica is used to form the core and the cladding layers. To deposit the layers, flame hydrolysis deposition (FHD) followed by high-temperature compaction and annealing steps is widely used. This method was adopted from fiber production and successfully applied to the fabrication of two-dimensional waveguide structures. The chemical vapor deposition (CVD) methods used in electronic chip manufacturing, such as low-pressure CVD, atmospheric-pressure CVD, or plasma-enhanced CVD (PECVD), are now preferred for deposition. Advantages in scalability and ease of parameter controllability favor their use and future deployment. The higher refractive index of the core

layer relative to that of the cladding layers is achieved by doping with germanium, phosphorus, or titanium. Rectangular or quadratic channel waveguide structures with optical propagation losses as low as 0.01 dB/cm, very small birefringence of the order of 10^{-5}, and, consequently, small polarization sensitivity can be fabricated. Because the shape of the optical mode is well matched to standard single-mode fibers, such waveguides can easily be coupled by aligning the flat waveguide end-facet with the cleaved fiber end and fixing the joint with an index-matching epoxy to minimize Fresnel reflections. This method can also be used for coupling arrays of fibers positioned in silicon V-grooves, and it routinely results in losses as low as 0.1 dB/point.

The relative difference of the refractive indexes between the core and the cladding layers—the so-called index contrast $\Delta = (n_{core} - n_{cladding})/n$—is an important parameter for controlling many optical properties of waveguides. In the conventional fiber-matched approach, typical values of $\Delta = 0.3\%$ are used, and the contrast can be influenced by the doping concentration [7–9]. The index contrast determines the size of the mode field and, hence, the minimum size for single-mode operation. Moreover, it is linked to the minimum bending radius for a waveguide below which optical radiation losses occur. With a Δ of 0.3%, radii of curvature of about 20 mm are possible before the onset of radiation losses; similarly, optical fibers can be curled to these dimensions before bend losses are observed. For higher values of Δ, accordingly smaller bend radii can be achieved. This means that integrated waveguide components with bent structures will have large chip dimensions, which limits a low-Δ technology in terms of integration density.

In this paper we present an overview of means to fabricate waveguides with much higher index contrast by using silicon oxynitride (SiON) core and silicon oxide cladding layers. By using well-established PECVD methods to deposit the layers on thermally oxidized silicon wafers, we achieve a large flexibility in waveguide design [10–12]. The nitrogen-to-oxygen ratio in the core layer can be varied continuously and over a significant range: from silicon oxide having a refractive index of 1.45 at one extreme to silicon nitride having a refractive index (or simply "index") of almost 2 at the other. Hence, the index contrast of the waveguide can be adjusted, ranging from the low contrast of fiber-matched processes to the high contrast of the waveguides of compound semiconductor structures. We expect this flexibility in index-contrast control to be an important advantage for future applications, for which it is anticipated that hybrid integrated electro-optical components will be assembled on a low-cost substrate optically connected via SiON waveguides with integrated mode converters. Here we focus on the clear advantage of higher-index-contrast

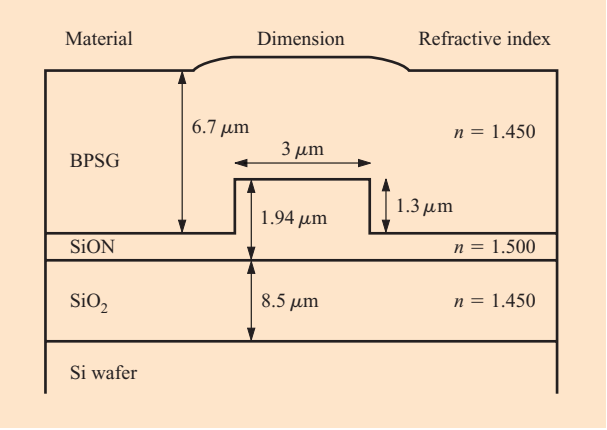

Figure 2

Schematic cross section and target design parameters of high-index-contrast SiON/SiO_2 waveguide. Note that all indices are given for TE-polarized light at a wavelength of 1550 nm. From [13] (Figure 1), with permission; © 2003 Springer-Verlag.

waveguides, specifically on the possibility of fabricating more complex, integrated optical devices in a compact way. Fabrication of well-established individual components such as phased-array WDM multiplexers on a smaller chip size is desirable, but does not yet justify the effort because the main share of the final costs lies in the fiber-to-chip alignment. Once a larger number of optical functions are integrated on a single chip in a compact way, the relative expenses of packaging should be reduced. The advantages of planar integrated functions fabricated using chip-manufacturing processes are beginning to appear, and deployment beyond the high-end WAN and MAN systems into the larger-volume customer-premises-area networking domain is expected. For the demonstration devices described in this paper, the index contrast was fixed at a value of about 3.3%, which corresponds to an atomic fraction of 7 to 8% of nitrogen in silicon oxide. By using a ridge-type waveguide cross section, as shown schematically in **Figure 2**, minimum bending radii of 0.8 mm with barely measurable radiation loss could be achieved. Furthermore, we describe dynamically reconfigurable planar integrated optical filter functions that can adjust the amplitude and/or the phase of the optical signals in a network node. As an example of a finite-impulse response (FIR) filter, we describe a dynamic gain-flattening filter for optical amplifiers, and as an example for an infinite-impulse response filter (IIR), we describe a CD compensator.

Planar waveguide SiON fabrication

The schematic cross section showing the layer structure and the design parameters of a high-index-contrast SiON

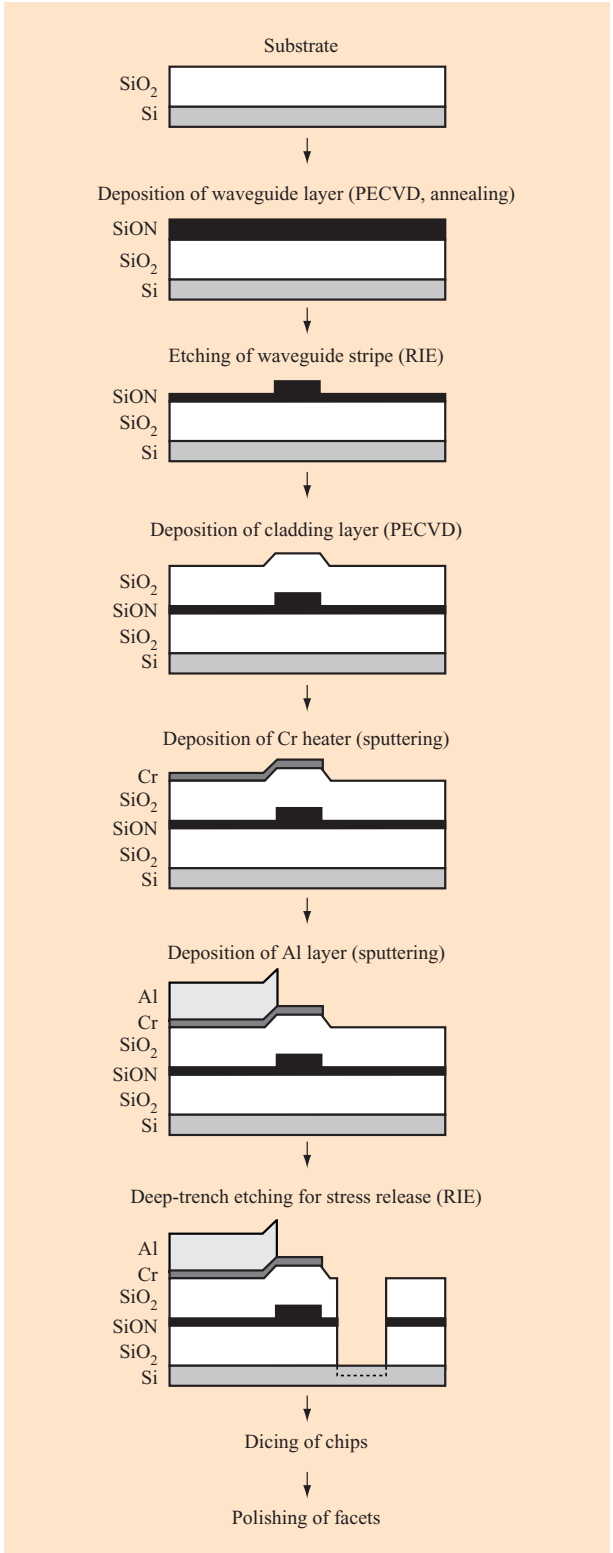

Figure 3

Fabrication process flow for high-refractive-index contrast SiON/SiO_2 waveguide structures. From [10], with permission.

waveguide is depicted in Figure 2. The SiON core layer is sandwiched between a lower cladding of silicon dioxide (SiO_2) and an upper cladding of boron phosphorus-doped silicate glass (BPSG). By using a SiON core with 7 to 8 mol% nitrogen, an absolute index contrast of 0.05, corresponding to $\Delta = 3.3\%$, is achieved. A minimum bending radius of 0.8 mm with barely measurable radiation loss and a 0.55 mm radius with less than 0.1 dB for a 90° bend have been demonstrated.

The fabrication process flow for SiON-based planar optical-waveguide devices, as described in [10], is illustrated in **Figure 3**. The lower cladding layer is formed by thermal oxidation of a 4-in. Si(001) substrate to a thickness of 8.5 μm. The SiON core layer is then deposited by PECVD, followed by an annealing step at a temperature of 1145°C, mainly to reduce optical propagation losses. The waveguide stripe pattern is defined by optical contact lithography and transferred to the SiON layer by reactive-ion etching (RIE) using a mixture of trifluor-methane (CHF_3) and oxygen (O_2). The SiON core layer is etched to a depth of 1290 nm. This etching process is anisotropic, and it produces vertical sidewalls that guarantee precise control and good reproducibility of the geometry and, accordingly, of the effective lateral index contrast of the waveguide structure. After the photoresist mask is stripped, the waveguide pattern is overgrown with 6.7 μm of BPSG as an upper cladding layer. This layer is formed by PECVD using SiH_4, N_2O, PH_3, and B_2H_6 as gaseous precursors, followed by an annealing step for layer consolidation. BPSG was chosen as the upper cladding because of its good gap-filling capability between closely spaced waveguide ridges, as they typically occur in directional couplers. The final fabrication step is to separate the individual device chips with a conventional dicing saw. The waveguide facets are polished to optical quality using an automated lapping and polishing tool. The remaining roughness of the facets, as measured by atomic force microscopy, is less than 26 nm. The thermo-optical effect of a typical SiON-based planar waveguide is measured to be $dN_{\text{eff}}/dT = 1.2 \times 10^{-5}$ °C^{-1}, which is typical for glass-type materials.

The SiON core layer determines the waveguide properties to a significant extent, and it is a major differentiator between our high-index-contrast approach and the standard lower-index-contrast approach. The deposition, annealing, and characterization of the SiON core layers are therefore described in this section in greater detail.

The SiON layers are deposited using a standard parallel-plate PECVD system. The upper gas "shower-head" electrode is powered at a frequency of 13.56 MHz. The bottom substrate electrode is grounded and can be heated to a temperature of 400°C. The system is pumped

by a combination of roughing pump and roots blower, and the pressure can be regulated independently of the gas influx. The gas consists of a mixture of 2% silane (SiH_4) in helium (He), nitrous oxide (N_2O), and ammonia (NH_3).

Several parameters such as gas flow rates, pressure, temperature, and power density have been varied to calibrate the deposition rate and the associated refractive index. Thin (~140 nm) SiON layers were deposited on silicon. The index and layer thickness were measured with an ellipsometer at a wavelength of 632.8 nm, and the experimental measurement accuracy was about ±0.0015 and ±0.5 nm, respectively. **Figure 4** shows the dependence of the index on the N_2O/SiH_4 gas-flow ratio for four different flow levels of NH_3, a pressure of 1 torr, an rf power of 15 W (corresponding to a power density of ~0.04 W/cm^2), and a substrate temperature of 400°C. The total gas flow of 750 sccm for 2% SiH_4/He and N_2O was kept constant. The index for the as-deposited SiON layers could be varied continuously between 1.46 and 1.56, which was the range of interest for our waveguide applications. A target index value in this range could be achieved either with or without NH_3 by adjusting the gas-flow ratio of N_2O and SiH_4 accordingly. Higher refractive indices up to values of 2.0 are possible by using a lower N_2O/SiH_4 ratio or a higher NH_3 flow, but this is not relevant to our applications at present. Deposition rates of 40 nm/min are typically achieved for this parameter field.

Because of the use of hydrogenated precursors, the as-deposited SiON layers contain a significant amount of hydrogen in the form of N–H bonds that cause propagation losses in the waveguides. The characteristic absorption frequency of the N–H stretching vibration is at a wavelength of 3.0 μm (wavenumber 3350 cm^{-1}) with its first overtone at 1.5 μm. The N–H stretching vibration is therefore the main cause of absorption losses in the wavelength region of interest, i.e., from 1529 to 1580 nm. The hydrogen content of the SiON layer and the corresponding absorption loss can be reduced by high-temperature annealing.

A Fourier transform infrared (FTIR) spectrum of an as-deposited 2-μm-thick SiON layer is shown in **Figure 5**. The characteristic modes of the tetrahedral SiO_4 groups near wavenumber 800 cm^{-1} (stretching), 1100 cm^{-1} (bending), and 470 cm^{-1} (bending) are indicated [14]. The absorption peak at 3350 cm^{-1} is due to the N–H stretching vibration. The oscillatory background is influenced by the finite thickness of the SiON layer. The inset in the figure shows the absorbance near 3500 cm^{-1} after background correction. The absorbance due to the N–H bond is reduced significantly after the use of annealing steps in the range of 1100°C for a few hours in a nitrogen atmosphere as part of our "standard" process.

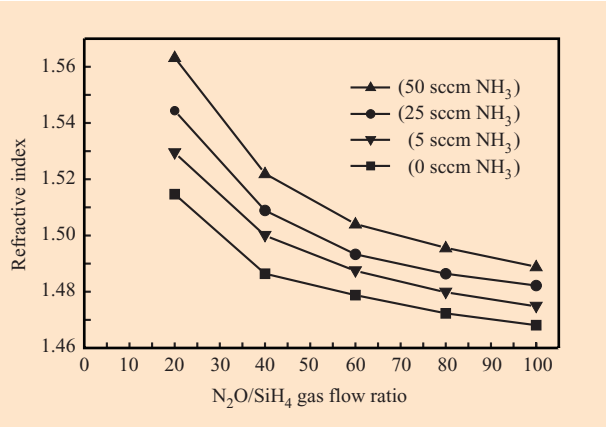

Figure 4

Refractive indices of thin (~140 nm) SiON films at several PECVD gas flow levels, measured with an ellipsometer at a wavelength of 632.8 nm. The N_2O/SiH_4 gas-flow ratio was calculated using the SiH_4 flow of the SiH_4/He mixture.

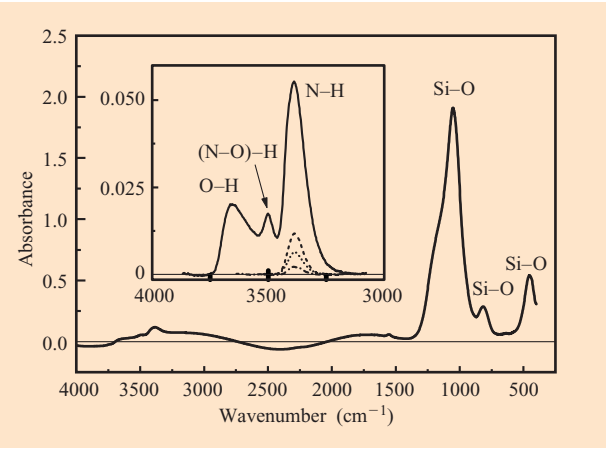

Figure 5

FTIR absorbance spectrum of an as-deposited 2-μm-thick SiON layer. The fundamental frequencies of tetrahedral SiO_2 are indicated. The inset shows an enlargement of the spectrum after background correction for different annealing conditions. The O–H and N–H stretching vibrations are indicated.

The absorbance of the N–H bond is currently being investigated in more detail, and a modified process which results in its reduction to below the detection limit will be described in a subsequent publication.[1]

A quantitative composition analysis of the hydrogen incorporation into SiON layers is obtained with Rutherford

[1] I. Meijer, IBM Research Division, Zurich Research Laboratory, CH-8803 Rüschlikon, Switzerland, unpublished results.

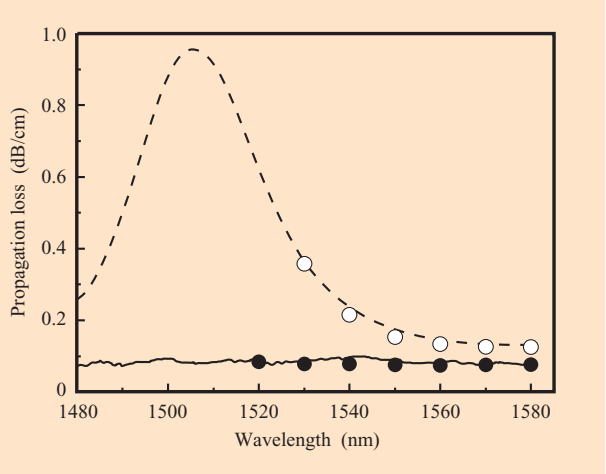

Figure 6

Wavelength-dependent loss of SiON channel waveguides fabricated using standard and modified processes (dashed and solid curves, respectively). Measurements were carried out between 1480 and 1580 nm on straight sections of the waveguides using a tunable wavelength laser source, and at several discrete wavelengths using ring resonators (as denoted by the open and solid circles, respectively).

backscattering (RBS). **Table 1** summarizes the results for the as-deposited and annealed layers. The hydrogen content in the as-deposited SiON layers is reduced from 0.16 ± 0.01 to 0.01 ± 0.01 because of the thermal annealing step at 1145°C. Note that the nitrogen content was about 0.08 ± 0.01 for both the annealed and the as-deposited samples. Similar results for the nitrogen concentration have been obtained from depth profiling, using Auger electron spectroscopy.

The annealing step at 1145°C results in an increase of the refractive index of the SiON layers from 1.4970 to 1.5170 as measured at a wavelength of 632.8 nm. Concomitantly, the thickness of the layer decreases by about 10%, from 2.140 to 1.940 μm. These measurements were performed using the attenuated total reflection (ATR) method [15] to increase the measurement accuracy for the refractive index. The uniformity on a 4-in.-diameter wafer was about 8×10^{-4} and 120 nm for index and thickness, respectively.

The optical waveguide devices must be insensitive to the state of polarization of the propagating light. In general, this requirement is not fulfilled for the layer structure described above. The various deposition and annealing steps cause stress in the waveguide layers, which, under the additional influence of waveguide geometry, lead to optical birefringence in the devices. This birefringence has been successfully tuned to negligibly small values by two different methods: 1) By using RIE to etch deep trenches in regions close to the waveguide and by adjusting trench depth and length and the distance between trench and waveguide, zero birefringence can be achieved [8]. 2) By careful optimization of the deposition and annealing steps as well as of the BPSG composition, the accumulated material stresses can be adjusted to achieve zero birefringence. We have obtained optical birefringence values of less than 1×10^{-4} with both methods. This leads to a polarization-dependent wavelength shift of 0.1 nm in our devices, which is sufficient for the applications foreseen.

Table 1 Atomic fractions of individual elements of a 1-μm-thick $SiO_xN_yH_z$ layer, as deposited by PECVD and after annealing, and measured by RBS.† The values for hydrogen were obtained by hydrogen forward-scattering spectrometry (HFS†), using an H^+ beam at grazing incidence. The HFS technique is sensitive to hydrogen with an estimated atomic fraction accuracy of 0.01 in the SiON matrix.

Element	*Atomic fraction as deposited*	*Atomic fraction annealed*
Si	1.00	1.00
O (x)	1.90	1.90
N (y)	0.07	0.08
H (z)	0.16	0.01

†RBS/HFS measurements were performed in the RBS/HFS facility of the CAFI Institute, University of Applied Sciences, 2400 Le Locle, Switzerland.

The optical propagation losses in SiON channel waveguides were measured on their "straight" sections using a tunable wavelength laser. Measurements were carried out between 1480 and 1580 nm. Accurate absolute loss values, which are not affected by chip facet properties, were obtained by characterizing ring resonators with large bend radii [16]. **Figure 6** shows the spectral behavior of the propagation losses of SiON channel waveguides fabricated using the standard and modified processes. Use of the standard process resulted in some absorption centered at 1510 nm, which could be attributed to the presence of residual N–H bonds. For the longer wavelengths, losses of 0.1 dB/cm were typically measured. Use of the modified process[1] resulted in a reduction of the propagation loss to below 0.1 dB/cm across the full spectral range. Note that the detection limit of the propagation loss measurement is well below 0.1 dB/cm, and many other contributions—e.g., photon scattering at sidewalls—in addition to the N–H bond reduction are important.

Another important parameter is the coupling loss between an optical waveguide device and a single-mode fiber. In the conventional approach, waveguide cross sections between 6×6 and 8×8 μm^2 are used. Values of less than 0.1 dB per facet for the butt-coupling of such

[1] I. Meijer, IBM Research Division, Zurich Research Laboratory, CH-8803 Rüschlikon, Switzerland, unpublished results.

a waveguide to a standard single-mode (SSM) fiber have been achieved. In our high-index-contrast process, the mode fields are confined to a much smaller area because of the stronger guiding. Consequently the butt-coupling loss to an SSM fiber is typically 3.7 dB per facet. This unacceptably high value can be reduced by using mode converters [17] or specially designed lensed fibers,[2] both of which lead to a reduction of more than 2 dB per facet. A relatively simple alternative is to use an intermediate piece of a small-core but high-index-contrast fiber that is well matched to the mode field of the waveguides. The light from the waveguide is thereby coupled to the small-core fiber with a diameter of ~3.5 μm, which is then spliced to a standard single-mode fiber with a core diameter of 9 μm. A total coupling loss of 0.5 dB per facet has been achieved with this method.[3] To relax packaging tolerances further, it is possible to combine an on-chip mode converter with the intermediate small-core fiber.

Dynamic gain equalizer

The high-refractive-index contrast SiON waveguide process described above has been used to fabricate a broad range of optical components for applications in the communication window around 1550 nm. Compact WDM-phased array waveguide grating multiplexers of substantially smaller size than in index-matched silica-on-silicon structures have been demonstrated—for example, a 16-channel device merely 6×7 mm^2 in size. Moreover, novel components with higher functionality have been realized. In addition to thermo-optical channel switches with up to eight ports [18], we have demonstrated reconfigurable FIR and IIR filters. Our FIR demonstrators were operated as WDM add/drop filters [19, 20] to select one or more wavelength channels out of a WDM stream, as dynamic-gain or channel equalizers [21] to flatten the response of the WDM channels, and even as adaptive dispersion compensators to compensate dynamically for chromatic dispersion.

In the following we describe the optical FIR-filter concept for the example of a dynamically reconfigurable gain-equalizer filter. Such optical filters are required to flatten the gain spectrum of an erbium-doped fiber amplifier (EDFA) but can also be used in connection with Raman optical amplifiers. Power imbalances of the WDM channels must be corrected, and this can be done for every channel individually using a channel equalizer or a DEMUX/MUX combination with variable intervening optical attenuators [22]. If channel power nonuniformity is mainly due to the spectral gain profile of the optical amplifier, a gain equalizer based on an FIR filter may be a simple solution because it can take advantage of the correlation between channels. A dynamically reconfigurable equalizer enables a reaction on the gain spectrum of an optical amplifier that depends on optical pumping and signal input power conditions. Consequently, changes in the network load as well as amplifier performance can be countered by appropriate equalization responses.

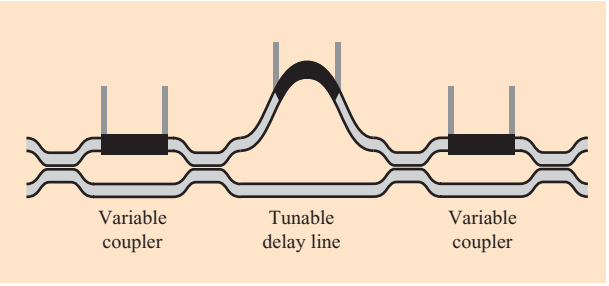

Figure 7

Basic building block of a tunable FIR-type optical filter consisting of two variable couplers and an intervening delay line.

The adaptive FIR filter is formed by cascading variable couplers and delay lines. Such a filter is also referred to as a resonant coupler (RC) or a cascaded Mach–Zehnder interferometer (MZI) [23]. A schematic drawing of the basic building block—an asymmetrical, tunable MZI—is shown in **Figure 7**. The heater resistor elements enabling thermo-optic control of the device are depicted by the dark stripes above the waveguides. The central delay line sets the free spectral range (FSR) of the interferometer response, which can be described by a harmonic function. The amplitude of the harmonic function can be varied by appropriately tuning the balanced arms of the variable couplers using the thermo-optic heater elements. Cascading many such stages results in a spectral response of the Fourier-series type. The highest harmonic contribution has a periodicity of FSR/N, where N is the number of MZI stages. The higher the number of stages, the better the ability to compensate an arbitrary gain spectrum.

Here we show the ability of a dynamic gain-equalization component (DGE) with seven stages, a seventh-order FIR filter. The FSR was chosen to be 40 nm, i.e., slightly larger than the typical bandwidth of an EDFA. Although the DGE consists of a chain of 15 tunable elements (eight variable couplers interspersed with seven tunable delay lines), it is only 32×4 mm^2 in size. For compactness, the layout is folded in such a way that the input and output waveguides are positioned next to each other. Folding was achieved by designing an asymmetrical MZI with a waveguide crossing. Experimentally we found that such crossings add less than 0.1 dB to the device-insertion

[2] Lensed fiber packaging was performed by Italtel Photonic Unit.
[3] Butt-coupling in V-groove packages was performed by Optospeed SA, Zurich, Switzerland.

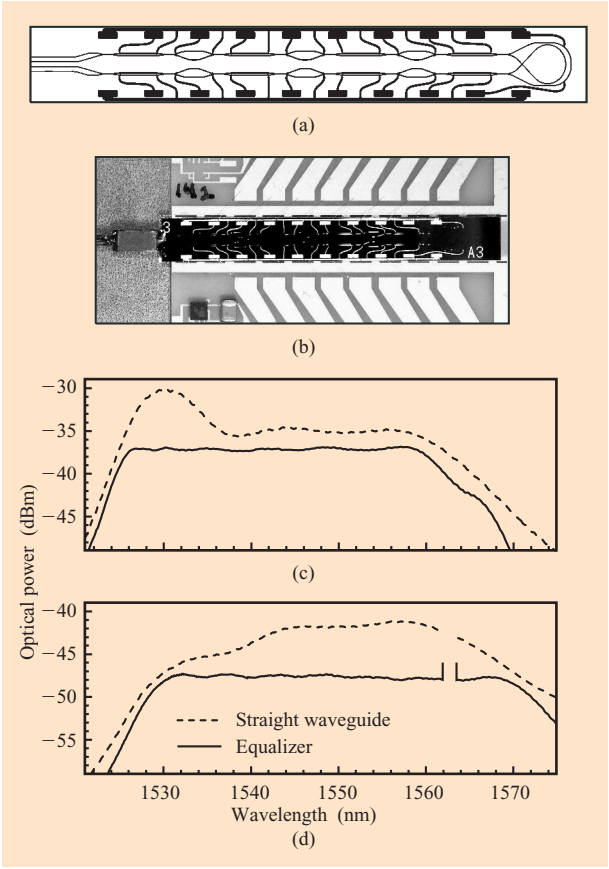

Figure 8

(a) DGE layout; (b) packaged DGE chip, mounted on an AlN heat spreader; (c) DGE flattened amplified spontaneous emission (ASE) response of an EDFA; (d) DGE flattened response of the distorted ASE of the same EDFA. From [13] (Figure 3), with permission; © 2003 Springer-Verlag.

loss. The device layout is shown in **Figure 8**, together with a photograph of a packaged device. Various filter responses of the seven-stage DGE and the strength of reconfigurability are also shown. A DGE SiON chip is shown mounted on an AlN subcarrier to ensure good thermal conduction to the housing. The former has electronic leads to enable an individual addressing of the thermo-optic heater elements on the DGE. The four fibers—two for the input and two for the filter output—are placed in a silicon V-groove array carrying the high-index intermediate fibers spliced to the standard fibers on 250-μm spacing. The array is actively aligned and attached with index-matched epoxy to the optical chip.[3] In addition to compactness, the folded design also reduces fiber-attachment costs because only one V-groove array has to be attached to the SiON chip. Fiber-to-fiber losses of the component of less than 3.5 dB have been measured.

The DGE is controlled by means of a PC-based electronic subsystem that addresses each heater element individually with appropriate power. A complete description of the device is required in order to calculate the heater power settings that correspond to the desired attenuation spectrum. A characterization procedure was developed that leads to a parameter-lookup table that is specific to the device. On the basis of this "feed-forward" procedure, the DGE can be reconfigured on a submicrosecond time scale. The agreement between the calculated and the actual device response was within 0.5 dB; a better accuracy (0.3 dB) was obtained by linking the device in a feedback loop.

The dashed curve in Figure 8(c) shows the amplified spontaneous emission spectrum of a wideband EDFA after propagation through a straight waveguide. The solid curve represents the experimentally optimized flattened spectrum. It shows a ripple of less than 0.4 dB over a range of 35 nm centered around 1543 nm. Subsequently, a strong input signal at 1563 nm was applied to the EDFA, which drastically altered the spectrum. The DGE was reconfigured and optimized using the same procedure, again resulting in a flat response over 37 nm with a ripple of less than 0.5 dB centered around 1550 nm [Figure 8(d)].

In addition to maximizing the accuracy of the FIR-filter curves, the polarization sensitivity of the component must be as small as possible. Minimization of the polarization-dependent loss (PDL) of the device for all possible filter curves is of utmost importance in practical applications. There are different effects that contribute to PDL, and all must be controlled by a careful processing of the SiON waveguides and by a clever FIR-filter design layout. The following sources of PDL have to be taken into account: 1) residual birefringence in the waveguide; 2) polarization dependence in the directional couplers; 3) stresses caused by burn-in of the heater elements (must be prevented or at least compensated for in the design); and 4) thermo-optic tuning (must be polarization-independent). The last is a very critical issue because the thermal tuning by the heaters can introduce stress effects due to the different thermal expansion coefficients of the waveguide structure. A careful optimization of the waveguide geometry led to polarization-independent tuning characteristics. All polarization effects were included in the software models that describe the gain equalizer. Excellent correlation between experimental curves and the model has been obtained, indicating that all of the significant effects were included and understood. Optimization of process technology and DGE design typically led to PDL values of

[3] Butt-coupling in V-groove packages was performed by Optospeed SA, Zurich, Switzerland.

less than 1.0 dB. With further process improvements and optimizations, we foresee a further reduction of the PDL values by at least a factor of 2. Active PDL reduction schemes offered by alternative phase shifters, such as those based on the use of liquid crystals, would be highly desirable, but a discussion of this possibility exceeds the scope of this paper.

Adaptive chromatic dispersion compensator

As we have seen, CD compensation in optical fiber networks becomes increasingly important with increasing bit rates to ensure good signal quality in data transmission. To obtain optimum dispersion compensation and to compensate for slowly varying dispersion fluctuations over time, a tunable dispersion filter is highly desirable. Basically, two approaches can be used in high-index planar waveguides: The FIR filters described in the preceding section can not only operate as tunable intensity filters but also enable moderate CD compensation over a wide frequency range [24]. On the other hand, IIR filters realized in the form of cascaded circular loop resonators allow large compensation in a thus far limited frequency range [25]. Waveguide loops or ring resonators with short circumference are required to obtain a wide filter repetition rate, or FSR. Hence, high-refractive-index waveguide structures with small bending radii are mandatory when fabricating IIR filters because the smaller the ring, the greater the achievable FSR will be. By cascading circular loops along a waveguide with individually tunable couplers and using heaters on the loops, adaptive dispersion compensators can be formed [24]. Such IIR filters exhibit sharp filter characteristics with only a small number of elements (rings). The coupling strength to the rings and the propagation and radiation losses of the loops determine the sharpness of the resonance. "Arbitrary" group delay curves can be synthesized by selectively tuning the individual ring resonances with respect to one another.

In the following example, we describe an IIR-type loop-resonator CD compensator. By cascading four ring loops along a waveguide, we have achieved widely tunable dispersion compensation over 50% of the bandwidth of the ring resonators. CD compensation was obtained with a linear group-delay response. Positive as well as negative CD values could be obtained by individually adjusting the heater currents of the four tunable couplers and the heater elements on each loop. Such optimization was achieved by monitoring the phase and amplitude response measured by a network analyzer and using a PC-controlled routine.

We have demonstrated linear dispersion compensation over FSR/2 in four-ring filters with 25-, 33-, and 50-GHz FSR [25]. The 50-GHz dispersion compensators were obtained by a compact design that exploited the minimum bending radius of 0.55 mm, leading to a loop circumference of 3.98 mm. Theoretically, up to 100 ps of group delay across 25 GHz and an absolute dispersion compensation of up to 500 ps/nm can be expected. **Figure 9** shows filter characteristics obtained over three times the FSR. By appropriate tuning we have obtained more than 80 ps of group delay. The excess loss was less than 4 dB. We achieved dispersion compensation ranging from −450 ps/nm to +450 ps/nm over more than 22 GHz of usable bandwidth. The ripple was irregular and very low.

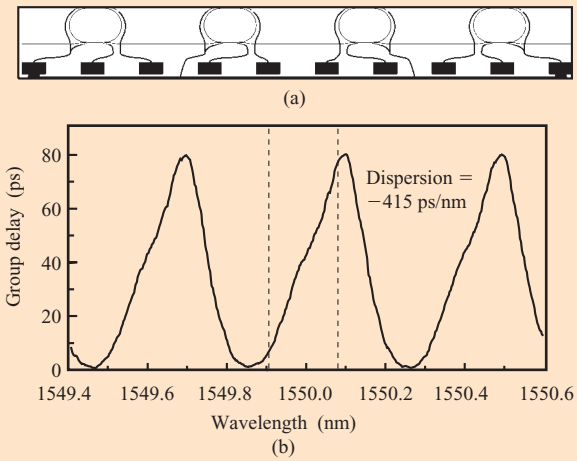

Figure 9

(a) Ring-resonator-based dispersion compensator layout; (b) a linear delay slope of −415 ps/nm with a usable bandwidth of 0.18 nm (22 GHz), as indicated by the two dotted lines. From [13] (Figure 4), with permission; © 2003 Springer-Verlag.

In such resonance-type devices, polarization-insensitive performance is even more important than in the FIR-filter example. The experimental data shown in Figure 9 were obtained for one polarization state. Because of the residual birefringence, CD compensation is slightly polarization-dependent. To overcome these difficulties, active waveguide birefringence control would be desirable for practical applications. Alternatively, this need could be addressed by applying a polarization diversity scheme in which the two polarization states are processed individually by two independent devices. Therefore, a polarization splitter and combiner pair would be required, but such components are easy to fabricate using the SiON waveguide process. As an additional advantage, the polarization diversity scheme enables the compensation of polarization-mode dispersion (PMD), the polarization-dependent signal delay in an optical network.

Concluding remarks

The high-refractive-index-contrast SiON waveguide process can be used to fabricate compact optical components as well as a wide range of tunable optical devices with enhanced functionality. This suggests that fabrication of integrated planar lightwave circuits for applications in telecommunication network nodes with optical cross-connect functionality may become possible. The refractive-index contrast chosen represents a good compromise between high integration density and low insertion loss. Because of the small bending radii (values as low as 0.55 mm), complex devices involving many optical building blocks can be realized. This advantage has been demonstrated by the fabrication of a seventh-order FIR filter for adaptive gain flattening. Moreover, small ring resonators with a free spectral range of up to 50 GHz and chromatic dispersion compensators in the form of an IIR filter have been fabricated. The adaptive thermo-optic filter configuration was achieved by means of an electronic subsystem with optimization algorithms that could be controlled via network management. The index contrast is small enough to allow the fabrication of low-transmission-loss waveguides using relatively simple processes. Low-loss coupling to a standard single-mode fiber is possible by using an intermediate section of small-core fiber, enabling cost-efficient array-to-SiON-chip coupling.

Acknowledgments

In realizing the SiON waveguide fabrication process and the adaptive optical filter functions with subsystem control, the dedicated work of the waveguide process technology, photonic device technology, and engineering services teams at the IBM Zurich Research Laboratory was instrumental and is gratefully acknowledged.

References

1. R. Morgan, "Options for High-Speed Transmission on Mixed-Grade Fiber Plant," *Lightwave*, pp. 140–148 (August 2000).
2. G. E. Keiser, "A Review of WDM Technology and Applications," *Optical Fiber Techn.* **5,** 3–39 (1999).
3. W. Denzel and B. Meekers, "Photonics in the Backbone of Corporate Networks—The ACTS COBNET Project," *Proceedings of the European Conference on Networks and Optical Communications* (*NOC '97*), IOS Press, Antwerp, Belgium, 1997, Part 3, pp. 225–232.
4. G. L. Bona, W. E. Denzel, B. J. Offrein, R. Germann, H. W. M. Salemink, and F. Horst, "Wavelength Division Multiplexed Add/Drop Ring Technology in Corporate Backbone Networks," *Opt. Eng.* **37,** 3218–3228 (December 1998).
5. J. P. Ryan, "WDM: North American Deployment Trends," *IEEE Commun. Mag.*, pp. 40–44 (February 1998).
6. M. K. Smit and C. van Dam, "PHASAR-Based WDM-Devices: Principles, Design and Applications," *IEEE J. Sel. Topics Quantum Electron.* **2,** 236–250 (1996).
7. Y. P. Li and C. H. Henry, "Silicon Optical Bench Waveguide Technology," *Optical Fiber Telecommun.* **IIIB,** 319–372 (1997).
8. M. Kawachi, "Silica Waveguides on Silicon and Their Application to Integrated-Optic Components," *Opt. & Quantum Electron.* **22,** 391–416 (1990).
9. P. Kersten and F. Bakthi, "Passive Optical Components for WDM Applications," *Integrated Optics Devices V*, G. C. Righini and S. Honkanen, Eds., *Proc. SPIE* **4277,** 54–68 (2001).
10. R. Germann, H. W. M. Salemink, R. Beyeler, G. L. Bona, F. Horst, I. Massarek, and B. J. Offrein, "Silicon Oxynitride Layers for Optical Waveguide Applications," *J. Electrochem. Soc.* **147,** No. 6, 2237–2241 (2000).
11. K. Wörhoff, B. J. Offrein, P. V. Lambeck, G. L. Bona, and A. Driessen, "Birefringence Compensation Applying Double-Core Waveguiding Structures," *IEEE Photon. Technol. Lett.* **11,** 206–208 (1999).
12. E. Bonnotte, C. Gorecki, H. Toshiyoshi, H. Kawakatsu, H. Fujita, K. Woerhoff, and K. Hashimoto, "Guided-Wave Acoustoopic Interaction with Phase Modulation in a ZnO Thin-Film Transducer on an Si-Based Integrated Mach–Zehnder Interferometer," *IEEE J. Lightwave Technol.* **17,** No. 1, 35–42 (January 1999).
13. G.-L. Bona, "Integrated Optical Planar Waveguide Components," *Microsystem Technologies: Micro- and Nanosystems—Information Storage and Processing Systems*, Springer-Verlag, 2003, Vol. 9, pp. 323–328.
14. C. M. M. Denisse, K. Z. Troost, F. H. P. M. Habraken, W. F. van der Weg, and M. Hendriks, "Annealing of Plasma Silicon Oxynitride Films," *J. Appl. Phys.* **60,** No. 7, 2543–2547 (1986).
15. S. Herminghaus and P. Leiderer, "Improved Attenuated Total Reflectance Technique for the Investigation of Dielectric Surfaces," *Appl. Phys. Lett.* **54,** No. 2, 99–101 (1989).
16. F. Horst, H. W. M. Salemink, R. Germann, B. J. Offrein, and G. L. Bona, "High Quality Ring Resonators in High Refractive Index Contrast SiON Waveguides," *Proceedings of the 1998 IEEE/LEOS Symposium, Benelux Chapter*, P. Demeester, R. Baets, A. Ackaert, and V. Masquelin, Eds., IEEE, Piscataway, NJ, 1998, pp. 33–36.
17. M. M. Spühler, B. J. Offrein, G. L. Bona, R. Germann, I. Massarek, and D. Erni, "A Very Short Planar Silica Spot-Size Converter Using a Nonperiodic Segmented Waveguide," *IEEE J. Lightwave Technol.* **16,** No. 9, 1680–1685 (1998).
18. E. Flück, F. Horst, B. J. Offrein, R. Germann, H. W. M. Salemink, and G. L. Bona, "Compact Versatile Thermo-Optical Space Switch Based on Beam Steering by a Waveguide Array," *IEEE Photon. Technol. Lett.* **11,** 1399–1401 (1999).
19. B. J. Offrein, G. L. Bona, F. Horst, H. W. M. Salemink, R. Beyeler, and R. Germann, "Wavelength Tunable Optical Add-After-Drop Filter with Flat Passband for WDM Networks," *IEEE Photon. Technol. Lett.* **11,** 239–241 (1999).
20. B. J. Offrein, R. Germann, F. Horst, H. W. M. Salemink, R. Beyeler, and G. L. Bona, "Resonant Coupler Based Add-After-Drop Filter in SiON Technology for WDM Networks," *IEEE J. Sel. Topics Quantum Electron.* **5,** 1400–1406 (1999).
21. B. J. Offrein, F. Horst, G. L. Bona, R. Germann, H. W. M. Salemink, and R. Beyeler, "Adaptive Gain Equalizer in High-Index-Contrast SiON Technology," *IEEE Photon. Technol. Lett.* **12,** 504–506 (2000).
22. C. R. Doerr, M. Capuzzo, E. Lakowski, A. Paunescu, L. Gomez, L. W. Stulz, and J. Gates, "Dynamic Wavelength Equalizer in Silica Using the Single-Arm Interferometer," *IEEE Photon. Technol. Lett.* **11,** 581–583 (1999).

23. K. Jinguj and M. Kawachi, "Synthesis of Coherent Two-Port Lattice-Form Optical Delay-Line Circuit," *IEEE J. Lightwave Technol.* **13,** 73–82 (1995).
24. C. Madsen and J. Zhao, *Optical Filter Design and Analysis: A Signal Processing Approach*, John Wiley & Sons, Inc., New York, 1999.
25. F. Horst, C. Berendsen, R. Beyeler, G.-L. Bona, R. Germann, H. W. M. Salemink, and D. Wiesmann, "Tunable Ring Resonator Dispersion Compensators Realized in High-Refractive-Index Contrast SiON Technology," *Proceedings of the 26th European Conference on Optical Communication* (*ECOC 2000*), Munich, Germany; post-deadline papers, paper 2.2, vde-Verlag, Berlin, Offenbach, 2000.

Received May 1, 2002; accepted for publication September 5, 2002

Gian-Luca Bona *IBM Research Division, Zurich Research Laboratory, CH-8803 Rüschlikon, Switzerland (glb@zurich.ibm.com).* Dr. Bona studied physics at the Swiss Federal Institute of Technology (ETH), where he received a Ph.D. degree in 1987 for his work on short-pulsed laser excited photoemission. In 1988, after postdoctoral work at the IBM Zurich Research Laboratory in the area of picosecond optical sampling of ultrafast devices, he became a Research Staff Member, working on quantum-well semiconductor lasers, with emphasis on the design and characterization of high-power and short-wavelength GaAs-based lasers. Since 1994, he has worked on the development of SiON/SiO_2 waveguides and planar lightwave circuits. Dr. Bona currently manages the photonic networking effort at the IBM Zurich Research Laboratory, covering areas ranging from single-mode adaptive integrated optical filter functions to parallel optical backplane applications as well as exploratory high-density optical interconnections using novel photonic bandgap concepts.

Roland Germann *IBM Research Division, Zurich Research Laboratory, CH-8803 Rüschlikon, Switzerland (ger@zurich.ibm.com).* Dr. Germann studied physics at the University of Stuttgart, where he received a Ph.D. degree in 1990. His dissertation deals with the dry etching of III–V semiconductors for the fabrication of nanostructures and DFB, and with the optical and electrical characterization of dry-etching-induced damage. In 1990, he joined the Zurich Research Laboratory as a Research Staff Member to work on the development of semiconductor lasers for optical data communication and storage applications. Since 1994 his work has been focused on the development of process technology for SiON-based planar optical waveguide circuits. Dr. Germann currently manages the process technology group within the photonic network program in the IBM Zurich Research Laboratory. He is a member of the German Physical Society.

Bert Jan Offrein *IBM Research Division, Zurich Research Laboratory, CH-8803 Rüschlikon, Switzerland (ofb@zurich.ibm.com).* Dr. Offrein studied applied physics at the University of Twente, The Netherlands, where he received a Ph.D. degree in 1994. His dissertation examined the measurement of optical nonlinearities and the design and realization of an all-optical switching device. From 1995 to 1999 he was a member of the optical networking group of the IBM Zurich Research Laboratory, working on the design and characterization of optical components for DWDM networks. In 1999, he joined the JDS Uniphase 980-nm pump laser facility in Zurich as a technical marketing engineer and yield engineer. A year later he returned to the IBM Zurich Research Laboratory to manage its photonic device technology group, which focuses on the design and characterization of state-of-the-art adaptive integrated optical components.